PALS/In Situ Multi-Campaign 800 m UTM Grid Brightness Temperature, Backscatter, and Soil Moisture Match-Up, Version 1

How to Cite These Data

As a condition of using these data, you must include a citation:

Colliander, A. 2016. *PALS/In Situ Multi-Campaign 800 m UTM Grid Brightness Temperature, Backscatter, and Soil Moisture Match-Up, Version 1*. [Indicate subset used]. Boulder, Colorado USA. NASA National Snow and Ice Data Center Distributed Active Archive Center. https://doi.org/10.5067/MPSKZBVINW95. [Date Accessed].

FOR QUESTIONS ABOUT THESE DATA, CONTACT NSIDC@NSIDC.ORG

FOR CURRENT INFORMATION, VISIT https://nsidc.org/data/NSIDC-0666

National Snow and Ice Data Center

TABLE OF CONTENTS

1 DETAILED DATA DESCRIPTION

1.1 Parameter or Variable

Parameters for this data set include:

- Brightness Temperature (TB), horizontally and vertically polarized (H-pol, V-pol)
- Normalized radar cross-section backscatter (H-pol, V-pol)
- Mean incidence angle (radiometer, radar)
- Volumetric soil moisture (in situ)
- Surface temperature (in situ, airborne)
- Soil temperature (1 cm, 5 cm depth)
- Vegetation Water Content (VWC) (in situ, airborne)
- Land cover class
- Crop type
- Clay fraction
- Sand fraction

Parameter units, values, and descriptions are provided in section 1.2.

1.2 File Contents

Table 1 summarizes the contents the data file, including parameters, units, and valid values.

For a more detailed description of the file contents, refer to the Data Fields section.

Table 1. Summary of File Contents

Column	Column Heading	Description	Unit	Valid Values
1	Year	Year	N/A	1999–2008
2	Month	Month of year	N/A	1–12
3	Day	Day of month	N/A	1–31
4	DOY	Day of year	N/A	1–365
5	Area	Area code (e.g. Walnut Creek = 070)	N/A	20–70
6	UTM-E	UTM easting of grid point	m	$3 \cdot 10^5$–$7 \cdot 10^5$
7	UTM-N	UTM northing of grid point	m	$3 \cdot 10^6$–$5 \cdot 10^6$
8	TB-V	Radiometer (L-band) V-pol calibrated brightness temperature (TB)	K	100–300

Column	Column Heading	Description	Unit	Valid Values
9	TB-H	Radiometer (L-band) H-pol calibrated brightness temperature (TB)	K	100–300
10	IA-Radiom	Radiometer beam mean incidence angle	Deg	35–45
11	S0-VV	Radar (L-band) VV-pol radar backscatter (sigma0, also referred to as S0)	dB	-25– -3
12	S0-HH	Radar (L-band) HH-pol radar backscatter (sigma0)	dB	-25– -3
13	S0-VH	Radar (L-band) VH-pol radar backscatter (sigma0)	dB	-37– -14
14	S0-HV	Radar (L-band) HV-pol radar backscatter (sigma0)	dB	-37– -14
15	IA-Radar	Radar beam mean incidence angle	Deg	35–45
16	SM	In situ soil moisture (where available)	cm^3/cm^3	0–0.6
17	Surf Temp-Air	Airborne infrared (IR) surface temperature (nadir)	°C	10–50
18	Surf Temp-Ground	In situ IR surface temperature (where available)	°C	10–50
19	Soil Temp-1cm	Soil temperature at depth of 1cm (where available)	°C	10–50
20	Soil Temp-5cm	Soil temperature at depth of 5cm (where available)	°C	10–50
21	VWC-Field	Vegetation Water Content from field sampling (where available)	kg/m^2	0–7
22	VWC-NDVI	Vegetation Water Content from Normalized Difference Vegetation Index (NDVI)	kg/m^2	0–7
23	Class	Land cover class based on MODIS-International Geosphere Biosphere Programme (IGBP)	N/A	0–254
24	Crop	Crop type	N/A	0–7
25	Clay	Clay percentage	%	0–100
26	Sand	Sand percentage	%	0–100
27	Flag 1	Performance flag 1: 1 when standard deviation, or STD(TB) < 4 K and STD(S0) < 2 dB, otherwise 0	N/A	0 or 1
28	Flag 2	Performance flag 2: 1 when STD(TB) < 8 K and STD(S0) < 4 dB, otherwise 0	N/A	0 or 1

1.3 Data Fields

1.3.1 Time Stamp (columns 1-4)

The data are time stamped based on the day of the PALS and in situ measurements; year, month of the year, day of the month and day of the year are included.

1.3.2 Areas and Coordinates (columns 5-7)

The study areas and corresponding grids of different campaigns are listed in Table 5. The grid points are defined at the center of the grid cell. The size of the study area corresponds to the grid of each particular study area. Each grid appears in column-wise order in the data and users should fill the matrix in column-by-column order.

For example, when V-pol brightness temperatures for any given campaign day such as 01 July 2002 is selected, the resulting vector can be ordered in a matrix. As listed in Table 5, the size of the SMEX02 matrix would be 10 by 43. Note that the coordinates on columns 6 and 7 can be used to check that the grid is formed correctly.

1.3.3 Brightness Temperature (columns 8-9)

L-band brightness temperature acquired with PALS. The configuration of PALS depends on the campaign. The data include vertically and horizontally polarized brightness temperatures. The flight altitude and antenna of the instrument vary from campaign to campaign. These differences have an effect on the consistency of the combined data record. Refer to Data Acquisition and Processing for details.

1.3.4 Normalized Radar Cross Section (columns 11-14)

L-band Normalized Radar Cross Section (NRCS) acquired with PALS. The configuration of PALS depends on the campaign. The data include the following polarizations:

- V-pol transmit/V-pol receive
- V-pol transmit/H-pol receive
- H-pol transmit/H-pol receive
- H-pol transmit/V-pol receive

The flight altitude and antenna of the instrument vary from campaign to campaign. These differences have an effect on the consistency of the combined data record. Refer to section 3 of this user guide.

1.3.5 PALS Incidence Angles (columns 10 and 15)

The incidence angle of the PALS measurements over each grid cell is obtained using the aircraft attitude.

1.3.6 In Situ Soil Moisture (column 16)

When a grid cell coincides with an in situ sample of soil moisture, the in situ soil moisture value is included in the data. Different methods are used in different campaigns which have an effect on the consistency of the combined data record. Refer to section 3 for details.

1.3.7 Infrared Surface Temperature from In Situ Measurements (column 17)

When a grid cell coincides with an in situ sample of surface temperature, the in situ surface temperature value is included in the data.

1.3.8 Infrared Surface Temperature from Airborne Measurements (column 18)

The measurement with the nadir-pointing infrared sensor mounted on the same aircraft as PALS.

1.3.9 Soil Temperature (columns 19 and 20)

When a grid cell coincides with in situ samples of soil temperature (at 1 cm and/or 5 cm depths), the in situ soil temperature values are included in the data.

1.3.10 Vegetation Water Content (VWC) from In Situ Measurements (column 21)

When a grid cell coincides with an in situ sample of VWC, the in situ VWC is included in the data.

1.3.11 Vegetation Water Content (VWC) from Satellite Measurements of NDVI (column 22)

Satellite-based NDVI resolved from acquisitions that were acquired in the time frame of the campaign are used to calculate VWC. The availability and quality of satellite observations vary from campaign to campaign. The difference in availability and quality has an effect on the consistency of the combined data record. Refer to section 3 for details.

1.3.12 Land Cover (columns 23 and 24)

The land cover classification follows the MODIS IGBP classes (see Table 2). The crop type is further specified for agricultural class (see Table 3).

Table 2. Land Cover Classes

Land cover class	**Code**
Water	0
Evergreen Needle leaf Forest	1
Evergreen Broadleaf Forest	2
Deciduous Needle leaf Forest	3
Deciduous Broadleaf Forest	4
Mixed Forests	5
Closed Shrub lands	6
Open Shrub lands	7
Woody Savannas	8
Savannas	9
Grasslands	10
Permanent Wetlands	11
Croplands	12
Urban and Built-Up	13
Cropland/Natural Vegetation Mosaic	14
Permanent Snow and Ice	15
Barren or Sparsely Vegetated	16
Fill Value	255

Table 3. Agricultural Class Crop Types

Crop Type	Code
N/A	0
Bare	1
Alfalfa	2
Corn	3
Soy	4
Wheat	5
Legume	6
Cotton	7

1.3.13 Soil Texture (columns 25 and 26)

Ancillary data sources provide the sand and clay fraction for the study areas. Refer to the Clay and Sand Percentages section in the Data Acquisition and Processing for details.

1.3.14 Performance Flags (columns 27 and 28)

The flags indicate the level of variance as standard deviation in the samples used to obtain a particular grid cell value.

1.4 Format

Data are in column-ordered ASCII text format. Refer to Table 1 for descriptions of each column in the data file, in addition to parameter units and valid values.

An associated Extensible Markup Language (XML) metadata file is also provided for the data file.

1.5 File and Directory Structure

Data are available via HTTPS in the following directory:
`https://n5eil01u.ecs.nsidc.org/SMAP_VAL/NSIDC-0666.001/`

Within this directory, there is one file:
`NSIDC0666_matchup_pals_grid_v107_111012.txt`

1.6 Naming Convention

The file is named according to the following convention:

`NSIDC0666_matchup_pals_grid_vXXX_YYMMDD.txt`

Where:

Table 4. File Naming Convention

Variable	Description
`NSIDC0666_matchup_pals_grid`	Identifies this data product
`vXXX`	3-Digit Version
`YYMMDD`	2-Digit Year, Month, and Day
`.txt`	Indicates this is a text file

File Name: NSIDC0666_matchup_pals_grid_v107_111012.txt

1.7 File Size

The file is approximately 3.5 MB.

1.8 Spatial Coverage

The following study areas correspond to the four different soil moisture campaigns:

Oklahoma: SGP99, CLASIC07

Southernmost Latitude: 34.91ºN
Northernmost Latitude: 35.21ºN
Westernmost Longitude: 98.67ºW
Easternmost Longitude: 97.83ºW

Iowa: SMEX02

Southernmost Latitude: 41.92ºN
Northernmost Latitude: 41.99ºN
Westernmost Longitude: 93.80ºW
Easternmost Longitude: 93.40ºW

Maryland: SMAPVEX08

Southernmost Latitude: 38.95ºN
Northernmost Latitude: 39.09ºN
Westernmost Longitude: 76.18ºW
Easternmost Longitude: 75.54ºW

1.9 Spatial Resolution

The spatial resolution is 800 m

1.10 Projection/Grid Description

Data are provided in Universal Transverse Mercator (UTM) World Geodetic System 1984 (WGS84) coordinates.

The study areas fall within the following UTM (WGS84) grid zones:

Oklahoma: 14 N
Iowa: 15 N
Maryland: 18 N

There are five separate grids in the data, each corresponding to a field campaign study area. Table 5 shows the number of rows and columns in each grid. In the file the data are ordered column-wise south to north, west to east. Thus, when data are searched for a given area on a given date, a collection of data points is returned which can be ordered as grid. This can be done by using the dimensions given in Table 5 and the 800 m grid spacing. Each grid appears in column-wise order in the data and users should fill the matrix in column-by-column order.

For example, when V-pol brightness temperatures for any given campaign day such as 01 July 2002 is selected, the resulting vector can be ordered in a matrix. As listed in Table 5, the size of the SMEX02 matrix would be 10 by 43 (the coordinates on columns 6 and 7 can be used to check that the grid is formed correctly).

Table 5. Description of Grids

Field Campaign	Study Area	Number of Rows in the Grid	Number of Columns in the Grid	Total Number of Data Points	Area Code
SMAPVEX08	Choptank (Maryland)	20	70	1400	020
SGP99	Little Washita (Oklahoma)	9	52	468	060
CLASIC07	Fort Cobb (Oklahoma)	4	35	140	050
CLASIC07	Little Washita (Oklahoma)	8	63	504	060
SMEX02	Walnut Creek (Iowa)	10	43	430	070

1.11 Temporal Coverage

Table 6 lists the temporal coverage of each campaign and the specific days measurements were collected. The temporal resolution varies for each campaign.

Table 6. Temporal Coverage and Resolution by Campaign

Campaign	Temporal Coverage	Temporal Resolution
SGP99	8–14 July 1999	8–9, 11–14 July
SMEX02	25 June–8 July 2002	25, 27 June 1, 2, 5–8 July
CLASIC07	11 June–6 July 2007	11–12, 19, 23–25 June 1, 3–6 July
SMAPVEX08	29 September–13 October 2008	29 September 2, 4, 6, 8, 10, 13 October

2 SOFTWARE AND TOOLS

Any word-processing program or Web browser is sufficient for viewing ASCII text files.

3 DATA ACQUISITION AND PROCESSING

3.1 Theory of Measurements

The data combine a suite of measurements collected in four different airborne soil moisture retrieval algorithm development campaigns: SGP99, SMEX02, CLASIC07, and SMAPVEX08. The goal of the campaigns was to obtain data that can be used to develop soil moisture retrieval algorithms based on microwave observations. Each campaign deployed an airborne instrument called PALS, the Passive Active L-band System, and this product combines the PALS observations with a set of ground truth data collected in those campaigns. For more details regarding theory of measurements, see Colliander et al. (2012).

3.2 Sensor or Instrument Description

With NASA support, the Jet Propulsion Laboratory (JPL) designed, built, and tested the PALS microwave aircraft instrument and deployed the instrument for measurements of soil moisture and ocean salinity (Wilson et al. 2001). PALS provides radiometer products, such as vertically and horizontally polarized brightness temperatures, and radar products, such as normalized radar backscatter cross-section for V-transmit/V-receive, V-transmit/H-receive, H-transmit/H-receive, and H-transmit/V-receive. In addition, it can also provide the polarimetric third Stokes parameter measurement for the radiometer and the complex correlation between any two of the polarized radar echoes (VV, HH, HV and VH). The following table provides the key characteristics of PALS:

Table 7. Description of the PALS instrument

Passive	Frequency	1.413 GHz
	Polarization	V, H, +45, -45
	Calibration stability	1 K (bias); 0.2 K (stability)
Active	Frequency	1.26 GHz
	Polarization	VV, HH, VH, HV
	Calibration accuracy	<2 dB (bias); 0.2 dB (stability)
Antenna	Half Power Beamwidth	20° (passive); 23°(active)
	Beam Efficiency	94%
	Directivity	18.5 dB
	Polarization isolation	> 35 dB

The PALS instrument was flown in the four major soil moisture experiments included in this data set: SGP99, SMEX02, CLASIC07 and SMAPVEX08 (Colliander et al. 2012). Beginning with CLASIC07, a new flat-panel antenna array was substituted for the large horns. The planar antenna consists of 16 stacked-patch microstrip elements arranged in a four by- four array configurations. Each stacked-patch element uses a honeycomb structure with extremely low dielectric loss at L-band to support the ground plane and radiating patches. The measured antenna pattern shows better than 33 dB polarization isolation, far exceeding the need for the polarimetric measurement capability. This compact, lightweight antenna has enabled PALS to transition to operating on small aircraft, such as the Twin Otter (Yueh et al. 2008).

PALS was mounted at a 40° incidence angle looking to the rear of the aircraft. The 3 dB spatial resolutions of the instruments at two potential altitudes are 500 m (due to 1000 m altitude, minimum for the radar operation) and 1500 m (due to 3000 m altitude, maximum for the radar). It is important to note that PALS provides a single beam of data along a flight track and that any mapping must rely upon multiple flight lines at a spacing of the footprint width.

The calibration of the PALS brightness temperature and backscatter during these four campaigns is described in Colliander et al. (2012).

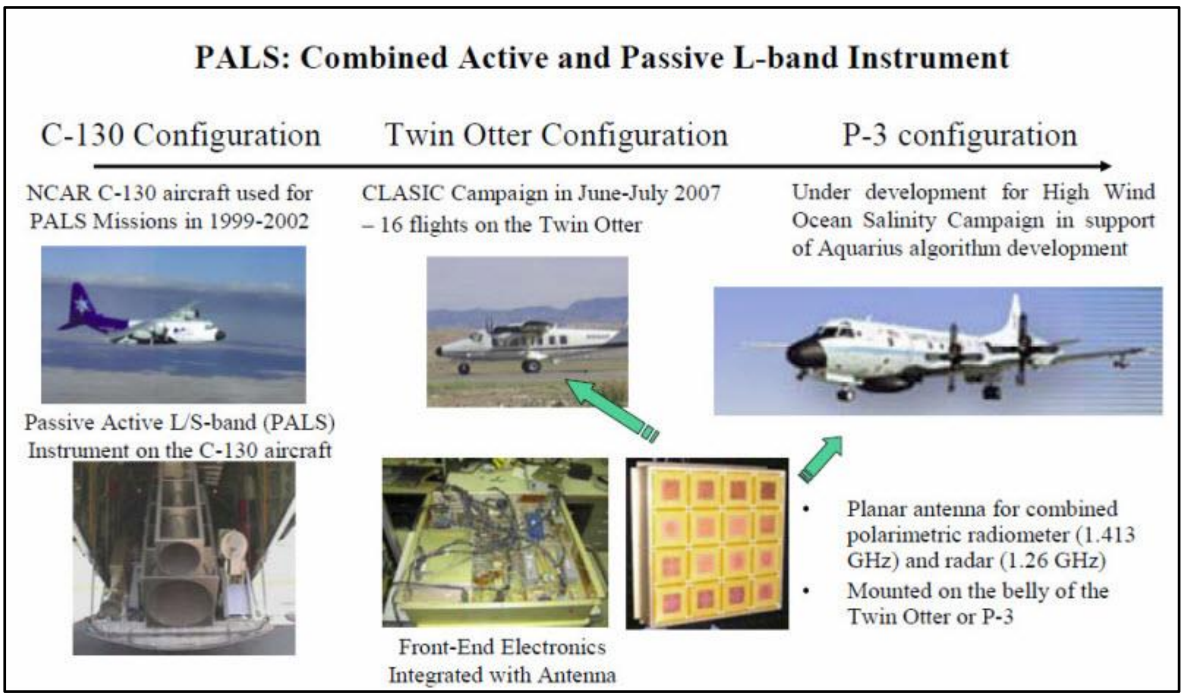

Figure 1. Active and Passive L-Band Instrument Descriptions

3.3 Derivation Techniques and Algorithms

The parameters in this data product were derived using the following techniques:

3.3.1 Brightness Temperature (columns 8-9)

The vertical and horizontal brightness temperature value is computed by averaging all brightness temperature values falling within a grid cell. The same procedure is applied to all campaigns. The standard deviation of the averaged set of data are also computed for performance evaluation and setting the performance flags.

3.3.2 Normalized Radar Cross Section (columns 11-14)

The radar cross-section value for different polarization combinations are computed by averaging (in linear scale) all radar cross-section values falling within a grid cell. The same procedure is applied to all campaigns. The standard deviation of the averaged set of data are also computed for performance evaluation and setting the performance flags.

3.3.3 PALS Incidence Angles (columns 10 and 15)

The incidence angle of the PALS measurements over each grid cell is obtained from the PALS data and averaged along with the brightness temperature and radar backscatter cross-section.

3.3.4 Volumetric Soil Moisture (column 16)

SGP99

Volumetric soil moisture estimates are based on a thermo-gravimetric method. The gravimetric soil moisture was measured at all in situ sites of the campaign on each day of the PALS flights. The match-up uses these values for corresponding days of the campaign. The bulk density of the soil of each in situ site was also determined (once), and that was used to determine the volumetric soil moisture corresponding to the gravimetric measurements.

SMEX02, CLASIC07, SMAPVEX08

Each in situ site was sampled with several soil moisture probe measurements on each day of PALS flights. The match-up uses the averaged value of these samples. The probe measurements were calibrated with occasional thermo-gravimetric measurements.

3.3.5 Infrared Surface Temperature: Airborne and In Situ (columns 17-18)

The physical temperature of the surface was measured by both airborne and handheld infrared sensor (for CLASIC campaign the airborne infrared data are to be processed).

The handheld measurement is applicable to ground skin temperature whereas the airborne measurement is applicable to the skin temperature of the field of view from the aircraft, which may include vegetation.

3.3.6 Soil Temperatures at 1 cm and 5 cm Depths (columns 19-20)

The physical temperature of the soil was measured in each campaign at the soil moisture in situ sites at depths of 1 cm and 5 cm on each day of PALS flights.

3.3.7 Vegetation Water Content (VWC): In Situ (column 21)

SGP99

Vegetation water content was determined one time for each in situ site during the campaign. The match-up data set uses this value for each day of the campaign.

SMEX02

Vegetation water content was determined for each in situ site 2 to 4 times during the campaign. The match-up uses the value which was obtained closest to the respective flight date.

CLASIC07

No in situ vegetation water content information is available.

SMAPVEX08

Vegetation water content was determined at eight sites one time during the campaign. The match up uses these values for these sites for each day of the campaign.

3.3.8 Vegetation Water Content (VWC): Satellite Derived (column 22)

VWC was retrieved from optical satellite measurements for some of the campaigns.

SGP99

NDVI data processing for VWC is forthcoming.

SMEX02

Several NDWI measurements over the course of the campaign were used to apply a model to map the VWC over the in situ sites. The VWC was interpolated to cover all measurement days. The match-up uses the interpolated VWC values for the respective flight dates.

CLASIC07

A one-time NDWI image was used to obtain the vegetation water content. The values are based on images obtained on 15 July 2007. The match-up uses this value for each day of the campaign. The conditions for VWC were less than optimal due to cloud cover over the test sites during the campaign. Caution is advised when interpreting these data.

SMAPVEX08

A one-time NDWI image was used to obtain the vegetation water content. The match-up uses this value for each day of the campaign.

3.3.9 Land Cover (columns 23-24)

The land cover over the in situ sites was determined based on the land classification maps, except for CLASIC07, in which case the in situ records were utilized. The crop classification of the agricultural fields is based on the in situ records.

3.3.10 Clay and Sand Percentages (columns 25-26)

The derivation of the clay and sand percentages for each campaign is explained below.

SMEX02

The SMEX02 data include the clay and sand fractions for the campaign region. The data are given in shape file (.shp) format. The shape files give the upper and lower limit of the fraction within each shape. For a given in situ site the clay and sand fractions are determined by averaging the upper and lower limits of the fractions given in the shapes falling within the defined pixel size from the coordinate of the site.

SGP99, CLASIC07

The clay and sand fractions are obtained from an online database hosted by the Earth System Science Center in the College of Earth and Mineral Sciences at The Pennsylvania State University. The data are from CONUS-SOIL, a multi-layer soil characteristics data set for the conterminous United States based on the USDA State Soil Geographic Database (STATSGO). A subset of these data was extracted for the SGP99 and CLASIC07 regions. The resolution of the data is 30 arc seconds. The data pixel closest to a given in situ site was selected to represent the clay and sand fractions of that in situ site.

SMAPVEX08

The clay and sand fractions for the SMAPVEX08 campaign were pre-processed by USDA-ARS based on the online database hosted by Pennsylvania State University. The data are from CONUS-SOIL, a multi-layer soil characteristics data set for the conterminous United States based on the USDA State Soil Geographic Database (STATSGO). The pre-processed data covers the SMAPVEX08 region in 100 meter resolution. The average of the clay and sand fraction within the defined pixel size was calculated to represent the respective in situ site.

3.3.11 Performance Flags (columns 27-28)

Two performance flags are given with the data. The flags indicate the level of variance in the samples used to obtain a particular grid cell value. They are determined based on the standard deviation (STD) computed from the set of brightness temperatures and radar cross-section samples falling within the given grid cell.

The first one indicates whether the STD of the brightness temperatures of both polarizations is less than 2 K and the STD of both HH-polarized and VV-polarized radar cross-sections is less than 4 dB. If so, the flag is 1. The flag is 0 in any other case.

The second one indicates whether the STD of the brightness temperatures of both polarizations is less than 4 K and the STD of both HH-polarized and VV-polarized radar cross-sections is less than 8 dB. If so, the flag is 1. The flag is 0 in any other case.

3.4 Error Sources

There are no exceptional error sources for this data set.

4 REFERENCES AND RELATED PUBLICATIONS

Bolten, J., V. Lakshmi, and E. Njoku. 2003. Soil Moisture Retrieval Using the Passive/Active L- and S-band Radar/Radiometer. IEEE Trans. Geosci. Rem. Sens. 41:2792-2801.

Colliander, A., E. G. Njoku, T. J. Jackson, S. Chazanoff, H. McNairn, J. Powers, and M. H. Cosh. 2016. Retrieving Soil Moisture for Non-Forested Areas using PALS Radiometer Measurements in SMAPVEX12 Field Campaign. Rem. Sens. of Environ. 184:86-100.

Colliander, A., T. J. Jackson, H. McNairn, S. Chazanoff, S. Dinardo, B. Latham, I. O'Dwyer, W. Chun, S. Yueh, E. Njoku. 2015. Comparison of Airborne Passive and Active L-Band System (PALS) Brightness Temperature Measurements to SMOS Observations During the SMAP Validation Experiment 2012 (SMAPVEX12). IEEE Trans. Geosci. Rem. Sens. 12:4.

Colliander, A., S. Chan, S. Kim, N. Das, S. Yueh, M. Cosh, R. Bindlish, T. Jackson, and E. Njoku. 2012. Long Term Analysis of PALS Soil Moisture Campaign Measurements for Global Soil Moisture Algorithm Development. Rem. Sens. of Environ. 121:309-322.

McNairn, H., T. Jackson, G. Wiseman, S. Belair, A. Berg, P. Bullock, A. Colliander, M. Cosh, S. Kim, R. Magagi, et al. 2015. The Soil Moisture Active Passive Validation Experiment 2012 (SMAPVEX12): Pre-Launch Calibration and Validation of the SMAP Satellite. IEEE Trans. Geosci. Rem. Sens., 53:5.

Narayan, U., V. Lakshmi, and E. Njoku. 2004. Retrieval of Soil Moisture from Passive and Active L/S Band Sensor (PALS) Observations during the Soil Moisture Experiment in 2002 (SMEX02). Rem. Sens. Environ. 92:483-496.

Njoku E., W. Wilson, S. Yueh, S. Dinardo, F. Li, T. Jackson, V. Lakshmi, and J. Bolten. 2002. Observations of Soil Moisture Using a Passive and Active Low Frequency Microwave Airborne Sensor during SGP99. IEEE Trans. Geosci. Rem. Sens. 40:2659-2673.

Njoku, E. G., and D. Entekhabi. 1996. Passive Microwave Remote Sensing of Soil Moisture. J. Hydrology, 184:101-129.

Wilson, W. J., S. H. Yueh, S. J. Dinardo, S. Chazanoff, F. K. Li, and Y. Rahmat-Samii. 2001. Passive Active L- and S-band (PALS) Microwave Sensor for Ocean Salinity and Soil Moisture Measurements. IEEE Trans. Geosci. Rem. Sens. 39, 1039-1048.

Yueh, S., S. Dinardo, S. Chan, E. Njoku, T. Jackson, and R. Bindlish. 2008. Passive and Active L-Band System and Observations during the 2007 CLASIC Campaign. Proc. IEEE IGARSS08. (2) II-241 - II-244, July 7-11, 2008.

5 CONTACTS AND ACKNOWLEDGMENTS

Andreas Colliander

Jet Propulsion Laboratory

California Institute of Technology

Pasadena, CA 91109 USA

6 DOCUMENT INFORMATION

6.1 Publication Date

February 2016

6.2 Date Last Updated

October 2020